Poloidal rotation, density asymmetries, and momentum confinement in tokamak experiments

W. M. Stacey and D. R. Jackson
Fusion Research Center and Nuclear Engineering Program, Georgia Institute of Technology, Atlanta, Georgia 30332

(Received 11 September 1992; accepted 26 February 1993)

Poloidal rotation speeds and density asymmetries are calculated for the deuterium and dominant carbon (oxygen) impurity ions in discharges in the Axially Symmetric Divertor Experiment (ASDEX) [*Proceedings of the 13th Conference on Plasma Physics and Controlled Fusion Research*, (International Atomic Energy Agency, Vienna, 1991), p. 325], Doublet III (DIII) [Nucl. Fusion **26**, 543 (1986)], Impurity Studies Experiment (ISX-B) [Nucl. Fusion **23**, 1017 (1983)], Joint European Torus (JET) [Nucl. Fusion **31**, 31 (1991)] and Tokamak Fusion Test Reactor (TFTR) (National Technical Information Document No. PB92177187) for which $v_\phi \sim v_{\rm th}$ for the ions. These poloidal rotation speeds and density asymmetries are used to evaluate the neoclassical gyroviscous model for the momentum confinement time. The rather good agreement with experimental momentum confinement times obtained over this wide range of plasma parameters provides a measure of confidence in the calculated density asymmetries and poloidal rotation, as well as demonstrating that neoclassical calculations can predict momentum confinement in tokamaks.

I. INTRODUCTION

Poloidal asymmetries in ion density and poloidal bulk rotation of ions in the central regions of tokamak plasmas are related topics which are of intrinsic interest in the understanding of tokamak physics and which also are of importance to the interpretation of toroidal rotation experiments because they determine the magnitude of the neoclassical (gyroviscous) toroidal angular momentum transfer rate.[1] A calculational model was recently developed[2] which now allows the calculation of poloidal density asymmetries and poloidal rotation in tokamak plasmas with strong toroidal rotation ($v_\phi \sim v_{\rm th}$).

The purposes of this paper are to apply the recently developed theory[2] to calculate the poloidal rotation and density asymmetries of the plasma and dominant impurity ions in a number of present and past tokamak experiments in which $v_\phi \sim v_{\rm th}$ for the ion species and to compare the predictions of momentum confinement times evaluated with these rotation speeds and density asymmetries against experimental momentum confinement times. There are no good measurements of density asymmetries and poloidal rotation in the center of tokamak plasmas with which our predictions may be directly compared, but the comparison of momentum confinement times provides an indirect comparison with experiment.

We note that there is a great deal of interest in poloidal rotation in the plasma edge region in connection with L–H mode transition studies and that measurements of poloidal rotation speeds in the plasma edge region have been made.[3–5] The theory[2] that we use is ordered for $v_\phi \sim v_{\rm th}$ and is thus not applicable to those measurements in which $v_\phi \sim \delta v_{\rm th}$ and in which radial gradient terms that we order out must be retained.

The paper is organized as follows. The calculational models are briefly summarized in Sec. II. The experimental parameters, the calculated poloidal rotation and density asymmetries, and the comparison of theoretical and experimental momentum confinement times are described in Sec. III. Related work is discussed in Sec. IV. A summary is provided in Sec. V.

II. THEORY

A. Poloidal rotation and density asymmetries

The fluid theory[2] which we will use models neutral beam injection (NBI) heated plasmas for which $v_\phi \sim v_{\rm th}$ and $E/B_\theta \sim O(v_{\rm th})$. Kinetic theory effects are accounted for in the viscosity and friction terms, following the Hirshman–Sigmar[6] moments approach.

The fluid particle equation

$$\nabla \cdot (n_j \mathbf{v}_j) = 0 \tag{1}$$

and the poloidal projection of the momentum balance equation

$$n_j m_j (\mathbf{v}_j \cdot \nabla)\mathbf{v}_j + \nabla p_j + \nabla \cdot \overleftrightarrow{\pi}_j + e_j n_j \nabla \Phi - n_j e_j \mathbf{v}_j \times \mathbf{B} = \mathbf{R}_j + \mathbf{M}_j \tag{2}$$

were solved self-consistently in the large-aspect-ratio approximation to determine the poloidal velocity v_θ and density asymmetries $\tilde{n}^c$ and $\tilde{n}^s$ in tokamak plasmas.

In deriving the equations, the poloidal dependences were expanded in the form

$$x(r,\theta) = \bar{x}(r)(1 + \tilde{x}^s \sin\theta + \tilde{x}^c \cos\theta) . \tag{3}$$

The solution for the (normalized) poloidal velocity $\hat{v}_{j\theta}$ was obtained from the poloidal component of Eq. (2) by integrating over θ, and may be expressed in the form

$$\hat{v}_{j\theta} = \frac{\text{driving}}{\text{damping}} = \frac{\text{driving}}{\text{viscosity} + \text{friction} + \text{inertia}} . \tag{4}$$

 0899-8221/93/061828-08$06.00

In the above equation, driving (the driving force) is given by

$$\hat{M}_{j\theta}+\hat{v}_{jr}+\bar{\nu}^{*}_{jk}\sqrt{\frac{m_j}{m_k}}\,\hat{v}_{k\theta} -q^2\hat{v}^{ex2}_{j\phi}\left\{\frac{\tilde{\Phi}^s}{\epsilon}+\frac{f_j}{2\hat{v}^{ex}_{j\phi}}\left[\frac{\tilde{\Phi}^s}{\epsilon}\frac{\tilde{n}^s_j}{\epsilon}+\frac{\tilde{\Phi}^c}{\epsilon}\left(5+\frac{\tilde{n}^c_j}{\epsilon}\right)\right]\right\} \tag{5}$$

and the three damping terms are given by

$$\text{viscosity}=q^2 f_j\left\{1+\frac{5}{6}\frac{\tilde{n}^c_j}{\epsilon}+\frac{2}{3}\frac{\tilde{n}^s_j}{\epsilon}+\frac{1}{3}\left[\left(\frac{\tilde{n}^s_j}{\epsilon}\right)^2+\left(\frac{\tilde{n}^c_j}{\epsilon}\right)^2\right]\right\} +\frac{q^2 f_j}{2}\left\{\frac{\tilde{\Phi}^s}{\epsilon}\frac{\tilde{n}^s_j}{\epsilon}+\frac{\tilde{\Phi}^c}{\epsilon}\left(5+\frac{\tilde{n}^c_j}{\epsilon}\right)\right\}, \tag{6}$$

$$\text{friction}=\bar{\nu}^{*}_{jk}, \tag{7}$$

$$\text{inertia}=-q^2\hat{v}^{ex}_{j\phi}\left(\frac{\tilde{n}^s_j}{\epsilon}+\frac{\tilde{\Phi}^s}{\epsilon}\right). \tag{8}$$

We note that in the poloidal projection of the viscous stress tensor the parallel (η_0) component of the viscosity is the leading term and enters the above expression via terms containing f_j.

By taking the sin θ and cos θ moments of the poloidal component of Eq. (2), two equations (for each ion species) coupling $\tilde{n}^s_j$ and $\tilde{n}^c_j$ are obtained:

$$\left[\left(\frac{2}{3}f_j-\beta^2\bar{\nu}^{*}_{jk}\right)\hat{v}_{j\theta}\right]\frac{\tilde{n}^s_j}{\epsilon}-\frac{1}{2}\frac{\tilde{n}^c_j}{\epsilon} =-(\hat{v}^{ex}_{j\phi})^2+\frac{1}{2}\hat{\Phi}_j\frac{\tilde{\Phi}^c}{\epsilon}-\beta^2\bar{\nu}^{*}_{jk}\hat{v}_{j\theta}\frac{\tilde{n}^s_k}{\epsilon}, \tag{9}$$

$$\left[\left(\frac{2}{3}f_j-\beta^2\bar{\nu}^{*}_{jk}\right)\hat{v}_{j\theta}\right]\frac{\tilde{n}^c_j}{\epsilon}+\frac{1}{2}\frac{\tilde{n}^s_j}{\epsilon}=-f_j\hat{v}_{j\theta}-\frac{1}{2}\hat{\Phi}_j\frac{\tilde{\Phi}^s}{\epsilon} +\beta^2\bar{\nu}^{*}_{jk}\left(\hat{v}_{j\theta}-\sqrt{\frac{m_j}{m_k}}\,\hat{v}_{k\theta}\right)-\beta^2\bar{\nu}^{*}_{jk}\hat{v}_{j\theta}\frac{\tilde{n}^c_k}{\epsilon}-\beta^2\hat{v}_{jr}. \tag{10}$$

Equations (4)–(10) are generally applicable to any number of ion species if $\bar{\nu}^{*}_{jk}$ is understood to represent a sum over species $k\neq j$. We specialize to the case of a main plasma species (j) and a dominant impurity species (k). Thus Eqs. (4), (9), and (10) for each species constitute six coupled, nonlinear equations in the unknowns $\hat{v}_{j\theta}$, $\hat{v}_{k\theta}$, $\tilde{n}^s_j$, $\tilde{n}^s_k$, $\tilde{n}^c_j$, $\tilde{n}^c_k$ which must be solved numerically.

Some important dimensionless quantities, which enter the above equations, are defined as follows:

$$\epsilon\equiv\frac{r}{R},\quad \bar{\nu}^{*}_{jk}\equiv\nu_{jk}qR/v_{\text{th}j},\quad \beta\equiv B_\theta/B_\phi,$$

$$f_j=\frac{\bar{v}^{*}_{jj}}{(\epsilon^{1.5}+\bar{v}^{*}_{jj})(1+\bar{v}^{*}_{jj})},\quad \hat{v}_{j\theta}\equiv\frac{\bar{v}_{j\theta}}{\beta v_{\text{th}j}},\quad \hat{v}^{ex}_{j\phi}\equiv\frac{\bar{v}^{ex}_{j\phi}}{v_{\text{th}j}},$$

$$\hat{v}_{jr}\equiv\frac{\bar{v}_{jr}}{\beta\delta_j v_{\text{th}j}},\quad \hat{M}_{j\theta}\equiv\frac{\bar{M}_{j\theta}}{\bar{n}_j m_j w_j v_{\text{th}j}\beta},\quad \hat{\Phi}_j\equiv\frac{e_j}{\frac{1}{2}m_j}\frac{\bar{\Phi}}{v^2_{\text{th}j}}, \tag{11}$$

where $v_{\text{th}j}$ is the thermal speed, $\hat{v}_{j\theta}$, $\hat{v}^{ex}_{j\phi}$, and $\hat{v}_{jr}$ are the normalized poloidal, experimental toroidal, and radial velocities of ion species j, respectively, $\hat{M}_{j\theta}$ is the poloidal momentum input, $\hat{\Phi}_j$ is the normalized electrostatic potential, ν_{jk} is the collision frequency, q is the safety factor, r and R are the minor and major radii, and $\omega_j\equiv V_{\text{th}\,j}/qR$ is the transient frequency.

B. Momentum confinement time

The neoclassical (gyroviscous) momentum confinement time is[7]

$$\tau^{\text{th}}_\phi\equiv\frac{2\pi R\int_0^a\langle Rnmv_\phi\rangle r\,dr}{2\pi R\int_0^a\langle R^2\nabla\phi\cdot\nabla\cdot\overleftrightarrow{\pi}_j\rangle r\,dr} =\frac{2R^2eB}{T}\left[\frac{h_{nTv}}{h_{nv}}\frac{\bar{m}_{\text{D}}}{m_{\text{D}}}\left(\frac{\tilde{\Theta}G}{Z}\right)^{-1}_{\text{eff}}\right], \tag{12}$$

where

$$\left(\frac{\tilde{\Theta}G}{Z}\right)_{\text{eff}} \equiv\int_0^a\left(\sum_{\text{ions}}\frac{\bar{n}_j}{\bar{n}_e}\tilde{\Theta}_jG_j\right)n_eTv_\phi r\,dr\Big/\int_0^a n_eTv_\phi r\,dr \tag{13}$$

and it has been assumed that all ion species have a common temperature, T, and rotation velocity, v_ϕ, and that $m_j\simeq Z_jm_{\text{D}}$. The poloidal density asymmetry factor for each ion species is

$$\tilde{\Theta}_j\equiv\left(4+\frac{\tilde{n}^c_j}{\epsilon}\right)\left[-\hat{v}_{j\theta}(\hat{v}^{ex}_{j\phi})^{-1}\left(\frac{\tilde{\Phi}^s}{\epsilon}+\frac{\tilde{n}^s_j}{\epsilon}\right)+\frac{\tilde{\Phi}^s}{\epsilon}\right] +\frac{\tilde{n}^s_j}{\epsilon}\left[\hat{v}_{j\theta}(\hat{v}^{ex}_{j\phi})^{-1}\left(2+\frac{\tilde{\Phi}^c}{\epsilon}+\frac{\tilde{n}^c_j}{\epsilon}\right)-\frac{\tilde{\Phi}^c}{\epsilon}\right], \tag{14}$$

where the $\tilde{\Phi}^{c/s}$ are related to the $\tilde{n}^{c/s}$ via charge neutrality and the electron momentum balance.[2] When radial profiles have the form $[1-(r/a)^2]^{\alpha_x}$, the radial profile factors have the form

$$G\equiv-\frac{r}{\eta_{4j}v_{\phi j}}\frac{\partial}{\partial r}(\eta_{4j}v_{\phi j})=\frac{2(r/a)^2(\alpha_n+\alpha_v+\alpha_T)}{1-(r/a)^2} \tag{15}$$

and

$$h_{nv}\equiv\frac{n(0)v_\phi(0)a^2}{2\int_0^a n(r)v_\phi(r)r\,dr}=1+\alpha_n+\alpha_v,\ \text{etc.} \tag{16}$$

The experimental momentum confinement may be written as[7]

$$\tau^{ex}_\phi=\frac{2\pi R\int_0^{\bar{a}}\langle Rnmv_\phi\rangle r\,dr}{\Gamma_\phi} =\frac{2\pi^2a^2R^2n_{e0}m_{\text{D}}v_{\phi0}h^{-1}_{nv}}{\Gamma_\phi} =\frac{2\pi^2\bar{a}^2R^3n_{e0}\bar{m}_{\text{D}}\Omega^{ex}_{\phi0}}{\Gamma_\phi h_{nv}}, \tag{17}$$

TABLE I. Summary of machine and plasma parameters.

Machine	References	R (m)	$\bar{a}$ (m)	I_p (MA)	P_b (MW)	B_ϕ (T)	Parameters $v_\phi^{ex}(0)$ (10^7cm/sec)	$T_i(0)$ (keV)	T_i/T_e	$\bar{n}_e$ (10^{13}/cm^3)	z_{eff}	α_n	α_v	α_T
ASDEX	12 and 13	1.65	0.40	0.42	1.8	2.17	1.5	1.23	1.0	4.6	3.2	0.54	1.2	1.1
DIII	8 and 14	1.43	0.385	0.7	3.85	2.53	1.2	1.89	1.0	8.0	1.85	0.97	0.99	2.0
		1.44	0.38	0.71	6.1	2.53	1.6	2.23	0.97	8.0	2.0	0.96	1.1	1.9
ISX-B	9, 15, and 16	0.93	0.25	0.155	0.85	1.4	1.1	0.72	1.0	4.5	2.5	1.0	1.0	1.0
JET (H)	7 and 17	3.00	1.10	3.1	7.7	2.2	2.0	5.5	1.25	3.0	2.3	0.0	1.5	1.5
JET (L)		3.00	1.10	3.22	14.25	3.47	3.5	15.5	1.5	1.33	3.5	2.0	3.0	3.5–4.0
TFTR	10	2.45	0.79	1.1	11.6	4.75	6.2	26.0	2.2	2.0	3.1	1.0	3.9	4.3

where

$$\Gamma_\phi=\frac{\sqrt{2m_b}R_{\tan}P_b}{\sqrt{E_b}} \tag{18}$$

is the torque input from NBI, $R_{\tan}$ is the tangency radius, E_b is the neutral beam energy, m_b is the mass of the beam particles, n_{e0} is the central electron density, $\Omega_{\phi 0}^{ex}$ is the central angular frequency, and $\bar{m}_D$ is an effective mass which reduces to m_D for deuterium plasmas.[7]

III. ANALYSIS OF EXPERIMENT

A. Experimental parameters

We reviewed the literature to identify at least one discharge for each of the major present and past tokamak experiments in which $v_\phi \sim v_{\text{th}}$ and for which the experimental parameters required to calculate both the poloidal speeds and density asymmetries and the momentum confinement times were available or could be reasonably extrapolated. We were able to identify such discharges for Axially Symmetric Divertor Experiment[4] (ASDEX), Doublet III[8] (DIII), Impurity Studies Experiment[9] (ISX-B), Joint European Torus,[7] (JET), and Tokamak Fusion Test Reactor[10] (TFTR), which provides a wide range of experimental parameters. Information concerning some input parameters was unavailable, however, and a few assumptions were made and applied to all tokamaks: safety factor $q(r/a=0.5)=2$, since $q(0)\sim 1$ and $q(a)\sim 3$; $\beta=B_\theta/B_\phi=0.1$; $e\Phi/T_i=1$; radial velocities $\hat{v}_{jr}$ and $\hat{v}_{kr}=0$; poloidal beam momentum inputs $\hat{M}_{\theta j}$ and $\hat{M}_{\theta k}=0$; radial profile of the form $x(r)=x_0[1-(r/a)^2]^{\alpha_x}$, except for DIII, where a density pedestal was included. The value of $e\Phi/T_i=1$, was obtained for ISX-B[11] at a potential of 0.5 kV and an average ion temperature of 500 eV. Since measurements of electrostatic potential were not available for the other machines, the value of $e\Phi/T_i$ obtained for ISX-B was assumed to be a reasonable estimate for all machines. We did not find that the available data were sufficient to confidently evaluate the radial profile of $(n_i/n_e)\tilde{\Theta}_i G_i$ for deuterium and carbon. Thus we elected to evaluate $(\tilde{\Theta}G/Z)_{\text{eff}}$ given by Eq. (13) by calculating $(n_i/n_e)\tilde{\Theta}_i G_i$ for both species at $r/a=0.5$ and using this constant value over $0<r<a$. We estimate that this approximation introduces an $O(10\%)$ uncertainty into the calculation. The parameters that characterize the discharges analyzed in this paper are given in Table I.

A well-documented[12,13] deuterium discharge with a dominant carbon impurity and with $\Omega_{\phi 0}=9.1\times 10^4$ rad/sec was analyzed for ASDEX. The peaking factors for density, angular velocity, and electron temperature, Q_x,[12] were used to construct the profile parameters, α_x

$$Q_x\equiv\frac{x_0}{\langle x\rangle}=1+\alpha_x\,. \tag{19}$$

Due to the relatively high density in the case chosen for analysis, T_i and T_e were roughly equal.[13] Thus the ion temperature profile factor α_T was assumed to be approximated by the electron temperature profile factor calculated from Q_{T_e}.

The data for DIII were obtained for deuterium plasmas with a dominant oxygen impurity. Data covering a wide range of experimental parameters were available.[8] However, experimental momentum confinement times were only available[14] for plasmas with somewhat different characteristics. The experimental parameters[8] were averaged over similar discharges and scaled to obtain parameters for two discharges for which momentum confinement data were available. The first case was an average of the data from two similar shots at a current of about 0.7 MA and 3.9 MW NBI. The other case was an average of the data from two similar shots at 0.71 MA and 6.1 MW NBI. The ion temperatures were scaled using the relation

$$T=T_1\frac{P_b\tau_\phi n_{e1}}{P_{b1}\tau_{\phi 1}n_e}, \tag{20}$$

where the subscript 1 indicates values at $\bar{n}_e=8\times 10^{13}$ cm^{-3}. The scaling was necessary since the plots of experimental confinement times[14] were available only for $\bar{n}_e=8\times 10^{13}$ cm^{-3}, whereas $\bar{n}_e$ for the tabulated data was lower. Straight-line fits to the plots of experimental confinement times versus beam power were not justifiable; τ_ϕ^{ex} varied slightly with P_b. The ratio of $P_b\tau_\phi$ to $P_{b1}\tau_{\phi 1}$ was set to unity in Eq. (20). The central velocities were available for only specific sets of data, namely $P_b=3.7$, 5.0, and 5.9 MW. The velocities at $P_b=3.7$ and 5.9 MW and a major radius of 1.52 m were chosen to describe the two cases at

TABLE II. Poloidal rotation and density asymmetries.

Machine	D $\hat{v}_{j\theta}$	C(O) $\hat{v}_{k\theta}$	D $\tilde{n}^c_j/\epsilon$	C(O) $\tilde{n}^c_k/\epsilon$	D $\tilde{n}^s_j/\epsilon$	C(O) $\tilde{n}^s_k/\epsilon$	$(\tilde{\Theta}G/Z)_{\rm eff}$
ASDEX	−0.15	−0.35	0.064	0.38	0.0087	0.061	0.23
DIII (1)	−0.063	−0.17	0.057	0.45	0.011	0.040	0.17
DIII (2)	−0.11	−0.27	0.073	0.57	0.0073	0.12	0.30
ISX-B	−0.13	−0.32	0.075	0.46	0.030	0.037	0.29
JET (H)	−0.047	−0.073	0.035	0.21	−0.0049	0.045	0.05
JET (L)	−0.11	−0.075	0.028	0.17	−0.0056	0.024	0.12
TFTR	−0.12	−0.079	0.047	0.28	−0.0031	0.023	0.08

3.9 and 6.1 MW ($R\sim 1.43$ m). As mentioned, the density profile was parabolic-to-a-power plus a pedestal.

Analysis of ISX-B[9,15,16] began with determining the experimental toroidal velocity as a function of the neutral beam power. A straight-line fit to the data yielded

$$v_\phi=(8.5+2.4P_b)(10^6) \tag{21}$$

with P_b in MW and v_ϕ in cm/sec. In ISX-B, the study focused on hydrogen neutral beam coinjection in deuterium plasmas with a dominant carbon impurity. The central ion temperature for such a plasma is given by

$$T_i(0)=T_{\rm OH}(0)+C\frac{P_b}{\bar{n}_e}, \tag{22}$$

where $C=2.2\times 10^{-19}$ keV MW^{-1} m^{-3} and $T_{\rm OH}(0)=0.3$ keV. The experimental momentum confinement time was 17 ms at $P_b=0.85$ MW and $\bar{n}_e=4.5\times 10^{13}$ cm^{-3}. Using these parameters in Eqs. (21) and (22) yields $v_\phi^{ex}=1.1\times 10^7$ cm/sec and $T_{i0}=716$ eV. Parabolic profiles were assumed.

Data for JET[7,17] covered both H-mode and L-mode deuterium plasmas with a dominant carbon impurity. For most H-mode discharges $\tau_\phi^{ex}=200$–500 msec, and for most L-mode discharges $\tau_\phi^{ex}=100$–200 msec.[7] However, ranges of experimental confinement times do not sufficiently indicate the accuracy of the theoretical model. For this reason, an experimental confinement time was constructed for one H-mode and one L-mode shot using the available data[17] and Eq. (17). Using an average $R_{\rm tan}=1.515$ m [eight ion sources with $R_{\rm tan}=1.85$ m and eight with $R_{\rm tan}=1.18$ m (Ref. 7)], the experimental momentum confinement time was calculated from Eq. (17) to be 204 msec for the H-mode shot and 70 msec for the L-mode shot. Density profiles were flat in H-mode discharges and more peaked than parabolic in L-mode discharges. Velocity and temperature profiles varied from slightly more peaked than parabolic in H-mode discharges to parabolic to the fourth power in L-mode discharges.[7] We chose representative profiles to be consistent with these observations.

A hot ion-mode discharge, which included temperature, velocity, and density profiles for a deuterium plasma with a carbon impurity, was chosen for the analysis of TFTR.[10] Determination of experimental momentum confinement time proceeded as for JET, with $\Gamma_\phi=18.25$ N m in Eq.(17), yielding an experimental momentum confinement time of 44 msec. Profile factors were determined from the measured profiles.

B. Calculated poloidal rotation and density asymmetries

The calculated poloidal rotation speeds and density asymmetries are displayed in Table II and the dominant driving forces for these rotations and asymmetries are indicated in Table III. The j and k subscripts denote deuterium and carbon (oxygen), respectively. Here $\hat{v}_{j\theta}>0$ corresponds to rotation in the direction of the B_θ field, $\tilde{n}^s_j>0$ corresponds to an upward density shift, and $\tilde{n}^c_j>0$ corresponds to an outward density shift—all in a right-hand (r,θ,ϕ) coordinate system in which the toroidal field and the toroidal current are aligned.

The density asymmetries, defined as

$$\tilde{n}(r)\equiv[n(r,\theta)-\bar{n}(r)]/[\bar{n}(r)]\,, \tag{23}$$

are less than the inverse aspect ratio ϵ in all cases. While $\tilde{n}^c_k$ ranges from 0.17ϵ to 0.57ϵ, $\tilde{n}^c_j$ and $\tilde{n}^s_k$ are much smaller and range from 0.023ϵ to 0.12ϵ. The smallest density asymmetry is $\tilde{n}^s_j$, the magnitude of which is in the range of 0.0031ϵ–0.03ϵ.

As the main ion and impurity ion species rotate in the toroidal direction (i.e., along the minor axis), inertial effects increase the density of the ions on the outboard side of the tokamak. Evaluation of each term coupling the density asymmetries showed that the largest term contributing to both $\tilde{n}^c_j$ and $\tilde{n}^c_k$ was indeed the inertia. The in–out density asymmetries are positive and increase with increasing values of the toroidal velocity, as would be expected. The

TABLE III. Summary of dominant driving forces.

Asymmetry		ASDEX, DIII, ISX-B	JET, TFTR
D	$\hat{v}_{j\theta}$	viscosity	viscosity, inertia
C (O)	$\hat{v}_{k\theta}$	viscosity, friction, inertia	viscosity
D	$\tilde{n}^s_j$	viscosity	E_θ
C (O)	$\tilde{n}^s_k$	viscosity	viscosity, inertia
D	$\tilde{n}^c_j$	inertia	inertia
C (O)	$\tilde{n}^c_k$	inertia	inertia

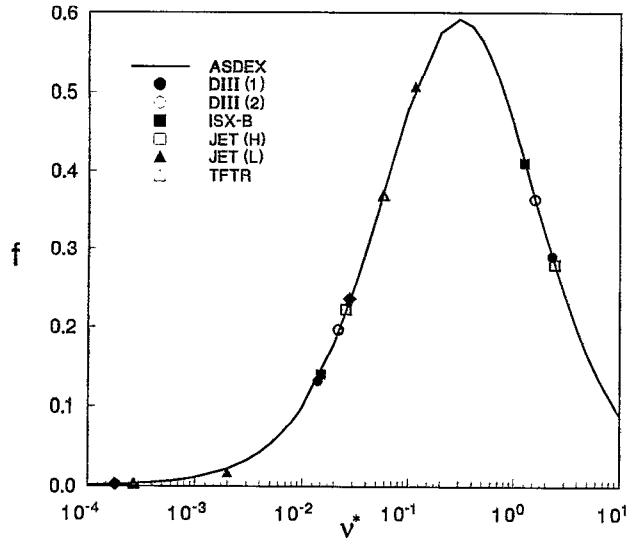

FIG. 1. Viscosity as a function of self-collision frequency.

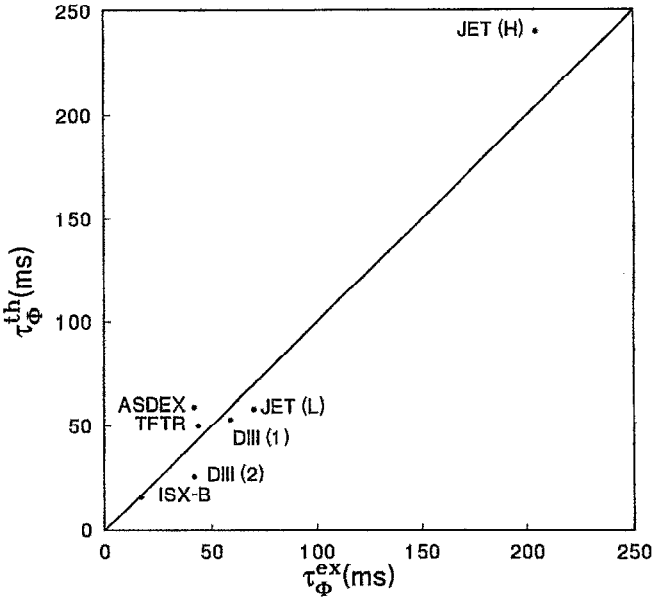

FIG. 2. Comparison of theoretical experimental momentum confinement times.

inertial term also contributed to the up–down impurity density asymmetry for TFTR and JET, with $\tilde{n}_k^3$ increasing with increasing v_ϕ.

The viscosity, which is a function of the self-collision frequency, drove the impurity ion up–down asymmetry in ASDEX, DIII, and ISX-B. The up–down asymmetry for the main ion species in JET and TFTR was driven by a combination of factors acting to drive a poloidal electric field. The up–down density asymmetries for the main ion species in ASDEX, DIII, and ISX-B and for the impurity ion species in all devices show an upward shift. However, the main ion species are shifted downward in JET and TFTR.

Analysis of Eq. (4) showed that the viscosity terms drove the poloidal velocity in all cases. The dependence of the poloidal velocities on the viscosity was nonmonotonic, a result which is consistent with the dependence of the quantity f on ν^* given by Eq. (11) and plotted in Fig. 1. The values of f, which determines the magnitude of the viscosity, for main deuterium ions and carbon (oxygen) ions is shown for the experiments in Fig. 1, with the leftmost value corresponding to the less collisional deuterium in each case. In general, the poloidal velocities were smallest for JET and TFTR. Furthermore, all values of v_θ were less than zero, indicating rotation opposite to the direction of B_θ for both species.

C. Comparison of theoretical and experimental momentum confinement times

The poloidal rotation speeds and density asymmetries in Table II were used to evaluate the quantities $\tilde{\Theta}_j$ of Eq. (14) and the effective poloidal asymmetry factor defined by Eq. (13), the latter of which was used together with the experimental parameters given in Table I to evaluate the theoretical momentum confinement time from Eq. (12). The poloidal asymmetry factor so calculated was $\sim O(0.1)$, with the major contribution coming from the deuterium ions. The experimental momentum confinement time was either evaluated using the data from Table I in Eq. (17) or taken as quoted by the experimental team, as discussed in Sec. III A. The theoretical and experimental momentum confinement times are compared in Table IV and Fig. 2. The rather good agreement provides some mea-

TABLE IV. Comparison of theoretical and experimental momentum confinement times.

Machine	I_p (MA)	P_b (MW)	B_ϕ (T)	$v_\phi^{ex}(0)$ (10^7 cm/sec)	$T_i(0)$ (keV)	$\bar{n}_e$ (10^{13}/cm^3)	τ_ϕ^{ex} msec	τ_ϕ^{th} msec
ASDEX	0.42	1.8	2.17	1.5	1.23	4.6	42	59
DIII	0.7	3.85	2.53	1.2	1.89	8.0	59	53
DIII	0.71	6.1	2.53	1.6	2.23	8.0	42	26
ISX-B	0.155	0.85	1.4	1.1	0.72	4.5	17	16
JET (H mode)	3.1	7.7	2.2	2.0	5.5	3.0	204	240
JET (L mode)	3.22	14.25	3.47	3.5	15.5	1.33	70	58–89
TFTR	1.1	11.6	4.75	6.2	26.0	2.0	44	50

sure of confidence that the poloidal speeds and density asymmetries given in Table II are correct, albeit it does not constitute a direct confirmation.

We note that our calculation is a first-principles, neoclassical calculation. The relatively good agreement with experiment over a wide range of devices then argues for a neoclassical explanation of ion momentum transport in tokamaks.

It is generally believed that momentum transport is anomalous. This belief has arisen because several experimental papers (e.g., Ref. 18) have stated that neoclassical *perpendicular* viscosity is too small by one–two orders of magnitude to explain observed momentum damping rates, an observation with which we agree. However, as elaborated in Ref. 1, there are two neoclassical mechanisms that damp toroidal momentum—perpendicular viscosity and gyroviscosity. It is the latter mechanism which we have now demonstrated, from first principle neoclassical calculations, to be of the proper magnitude to account for the momentum damping rates observed in a wide range of experiments. The agreement that we have obtained does not rule out the possibility that non-neoclassical (i.e., anomalous) mechanisms contribute to momentum transport, but it does obviate the necessity to posit such. To the extent that anomalous processes do enter into the determination of momentum confinement, the indirect experimental support for the correctness of the calculation of density asymmetries and poloidal rotation is weakened.

There are a number of studies in the literature of momentum confinement as a function of various experimental parameters (e.g., Refs. 7, 10, 12, 14, and 19) in some of which scalings of momentum diffusivity or momentum confinement with machine parameters, most notably current, have been inferred. While it would be of interest to check that Eq. (12), with the poloidal asymmetry factor of Eq. (14) evaluated using poloidal density asymmetries and rotation speeds calculated from Eqs. (4) and (9) and (10), could explain the inferred scalings, the plasma parameters needed to evaluate the latter equations for the different discharges are not documented in the literature, and such a study thus becomes beyond the scope of this paper and is best done by those associated with the experiments. We note that in at least one of these experimental studies,[14] the inferred dependence upon plasma current was directly due to the variation of radial profiles with plasma current. We further note that the dependence of momentum confinement on temperature given by Eq. (12) seems to be consistent with the data from a number of devices.[7,10,20] However, without an understanding of such correlations as exist between the plasma parameters involved in the scaling relations inferred from experiment and poloidal asymmetries, poloidal rotation and radial profiles involved in Eq. (12), we are unable to directly comment on the consistency of Eq. (12) with the experimentally inferred scaling with current (or with any other parameter).

Simultaneous measurements (e.g., Refs. 14 and 19) of ion thermal and momentum transport properties on machines suggest their correlation. This suggested correlation between ion thermal and momentum conduction has been cited as evidence that both are anomalous, since some anomalous theories predict heat and momentum conductivities that scale similarly with plasma parameters. This conclusion is somewhat weakened by the fact that classical Braginskii heat and momentum diffusivities also scale similarly with plasma parameters. In both cases, the theoretical magnitudes are quite different than the observed magnitudes. We have recently shown that, in the collisional region of strongly rotating tokamak plasmas, there is both a "rotational" ion energy flux[21] and a rotational ion momentum flux[22] which scale similarly and which scale like the gyroviscous momentum flux except with a different (but similar) poloidal asymmetry factor. Our calculations suggest that these rotational fluxes also could be responsible for the observed correlation. However, without further detailed analysis, it is not possible to reconcile our results with the suggested correlation between ion thermal and momentum conduction.

IV. RELATION TO OTHER WORK

There are literally no measurements of poloidal rotation or density asymmetries in the center of tokamak plasmas. As noted previously, there are several recent measurements[3–5,23] of poloidal rotation in the edge, but our ordering scheme ($v_\phi \sim v_{\rm th}$) is generally not applicable. Up–down impurity density asymmetries have been measured[24–29] in the edge of several tokamaks; again our ordering scheme is generally not applicable.

A number of authors[27,30–32] have pointed out the contribution of friction and inertia forces to driving asymmetries in the densities of very collisional ions. A self-consistent calculation[33,34] of toroidal and poloidal rotation and poloidal density asymmetries, similar to our model[2] but with a phenomenological representation of radial momentum transport instead of the neoclassical stress tensor, was made for ISX-B and PLT parameters some years ago. The deuterium poloidal rotation and density asymmetries obtained[34] are comparable to those given in Table II for ISX-B, but the high-Z impurity (titanium, tungsten) was calculated to have much larger poloidal rotation and density asymmetries than shown in Table II for carbon. This is consistent with the dependence of the calculation on collisionality reported previously.[2]

More recently, Kim *et al.*[35] have developed a neoclassical model for toroidal and poloidal rotation that is similar to the one[2] that we use. However, these authors do not treat the effect of poloidal density asymmetries on poloidal rotation, but do retain pressure gradient terms which order out in the $v_\phi \sim v_{\rm th}$ ordering of our model.[2]

Variations of Eq. (12) have been used to rather successfully predict[7,14,10,20] momentum confinement times in a variety of tokamaks. Heretofore, the poloidal asymmetry factor of Eq. (13), or some variant thereof, has been estimated instead of calculated. Our calculations of the poloidal asymmetry factors are quite close to the previously estimated values.

In a different vein, the calculations of this paper should resolve the controversy over neoclassical gyroviscous mo-

mentum transport, the salient remaining points of which we first summarize. Stacey and Sigmar[1] worked out the neoclassical stress tensor in toroidal coordinates and found that the gyroviscous contribution to the radial transport of toroidal angular momentum was proportional to the up–down asymmetry in toroidal velocity, which in turn depended on the up–down density asymmetry for the species in question. Based on their previous calculation[34] of $O(\epsilon)$ up–down density asymmetries for titanium/tungsten in ISX-B/PLT, they postulated that $O(\epsilon)$ up–down impurity density asymmetries could be present in tokamak experiments and showed that alone (without regard for the deuterium density asymmetry) would make the gyroviscous momentum transport the proper magnitude to explain the experimentally observed momentum damping.

Connor *et al.*[36] analyzed Eqs. (1) and (2) and argued from ordering considerations that the poloidal rotation would be, in essence, 0.1δ times smaller than the thermal speed, where δ is the gyroradius-to-gradient-scale-length parameter. From this argument they concluded that the gyroviscous momentum transport would be orders of magnitude too small to explain the experimentally observed momentum damping rates. Stacey[37] then summarized evidence for $O(\epsilon)$ impurity asymmetries and pointed out an apparent inconsistency in the Connor *et al.* ordering argument when $v_\phi \sim v_{\rm th}$.

Now that a first-principle, neoclassical calculation of the gyroviscous momentum damping rate has been performed, the "controversy" can be resolved. The model[2] used for the calculations of this paper is based on a consistent ordering when $v_\phi \sim v_{\rm th}$. Neoclassical theory predicts a (gyroviscous) momentum damping rate that is of the magnitude observed in tokamak experiments. This momentum damping is produced primarily by deuterium ion asymmetries of magnitude $\ll O(\epsilon)$, rather than by $O(\epsilon)$ carbon or oxygen asymmetries as suggested by Stacey.[37] The calculated poloidal rotation speeds are orders of magnitude larger than the values of 0.1δ times the thermal speed argued by Connor *et al.*[36] purely on the basis of (apparently inconsistent) ordering considerations.

V. SUMMARY

A recently developed neoclassical theory has been used to calculate the poloidal rotation and density asymmetries in ASDEX, DIII, ISX-B, JET, and TFTR. Using measured plasma parameters and a neoclassical model, the poloidal rotation velocity, the in–out density asymmetries, and the up–down density asymmetries were predicted for the deuterium and dominant carbon (oxygen) impurity species in these plasmas.

Adequate experimental data does not exist to allow a direct confirmation of the predictions. Thus the validity of the theory was confirmed indirectly by comparing theoretical momentum confinement times, which depend directly on the poloidal velocities and density asymmetries, with the experimental momentum confinement times.

Analysis showed that the main ion and impurity ion poloidal velocities were in the negative B_θ direction and depended on the plasma viscosity and the inertial effects of the toroidal rotation. For more collisional impurities, the poloidal velocity was also affected by friction. The up–down density asymmetries for both ion species were affected mainly by a combination of the viscosity and the up–down potential asymmetries, while the in–out density asymmetries depended on the toroidal velocity for both ion species. The magnitude of the poloidal rotation varied, for deuterium, from about $0.005v_{\rm th}$ to $0.015v_{\rm th}$ and, for carbon (oxygen) from about $0.007v_{\rm th}$ to $0.035v_{\rm th}$. The magnitude of the in–out density asymmetries varied, for deuterium, from about 0.03ϵ to 0.07ϵ and, for carbon (oxygen) from about 0.2ϵ to 0.6ϵ. The magnitude of the up–down density asymmetries varied, for deuterium, from about 0.003ϵ to 0.03ϵ and, for carbon (oxygen) from about 0.02ϵ to 0.1ϵ.

Using the calculated density asymmetries and poloidal rotation speeds to evaluate the poloidal asymmetry factors of the neoclassical gyroviscous theory, momentum confinement times were calculated which agreed with experimental values to within 6%–40%. This level of agreement provides (indirectly) some confidence that the predicted density asymmetries and poloidal rotation speeds are correct and demonstrates that a first-principles neoclassical calculation can predict ion momentum confinement over a wide range of experimental parameters. While this agreement does not exclude the possibility of anomalous momentum transport, it does obviate the necessity to posit such. Any anomalous effects would, of course, weaken the indirect support for the correctness of the calculated asymmetries.

ACKNOWLEDGMENTS

The calculations reported in this paper were performed as part of the M. S. thesis[38] of one of the authors (D.R.J), wherein greater detail may be found about the calculational procedures. The authors thank Dr. A. Kallenbach for providing additional data essential to the analysis of the ASDEX rotation data.

This work was supported in part by the U. S. Department of Energy under Grant No. DE-FG05-87ER51112 and in part by the Georgia Tech Fusion Research Center.

[1] W. M. Stacey and D. J. Sigmar, Phys. Fluids **28**, 2800 (1985).
[2] W. M. Stacey, Phys. Fluids B **4**, 3302 (1992).
[3] R. J. Groebner, K. H. Burrell, and R. P. Seraydarian, Phys. Rev. Lett. **64**, 3015 (1990).
[4] F. Wagner, F. Ryter, A. R. Field, G. Fussmann, J. V. Hofmann, M. E. Manso, O. Vollmer, R. Buchse, G. Dodel, A. Eberhagen, M. Endler, W. Englehardt, H. U. Fahrgach, O. Gehre, J. Gernhardt, L. Giannone, O. Gruber, H. J. Hartfuss, W. Hermann, E. Holzhauer, A. Kallenbach, O. Kardaun, F. Karger, O. Kluber, M. Kornherr, K. Lackner, R. Lang, J. Matias, H. M. Mayer, K. McCormich, V. Mertens, E. R. Muller, H. D. Murmann, J. Neuhauser, H. Niedermeyer, W. Poschenrieder, A. Rudyj, U. Schneider, R. Schubert, G. Siller, E. Simmet, F. X. Soldner, A. Stabler, K. H. Steuer, U. Stroth, N. Tsois, H. Verbeek, and H. Zohm, *Proceedings of the 13th International Conference on Plasma Physics and Controlled Fusion Research*, Washington, D. C. (International Atomic Energy Agency, Vienna, 1991), p. 277.
[5] Y. Miura, H. Aikawa, K. Hoshino, S. Kasai, T. Kawakami, H. Kawashima, H. Maeda, T. Matsuda, M. Mori, K. Odajima, H. Ogawa, S. Sengoku, M. Shimada, T. Shoji, N. Suzuki, H. Tamai, S. Tsuji, T. Yamamoto, T. Yamauchi, T. Fujita, A. M. Howald, A. W. Hyatt, K. Ida, A. W. Leonard, N. Ohyabu, S. Gunji, T. Hamano, K. Hasegawa, A. Honda, I. Ishibori, Y. Kashiwa, M. Kazawa, K. Kikuchi, F. Okano,

E. Sato, N. Seki, T. Shibata, T. Shiina, K. Suzuki, S. Suzuki, T. Tokutake, and S. Uno, *Proceedings of the 13th International Conference on Plasma Physics and Controlled Fusion Research*, Washington, D. C. (International Atomic Energy Agency, Vienna, 1991), p. 325.
[6]S. P. Hirshman and D. J. Sigmar, Nucl. Fusion **21**, 1079 (1981).
[7]W. M. Stacey, Nucl. Fusion **31**, 31 (1991).
[8]R. J. Groebner, W. Pfeiffer, F. P. Blau, K. H. Burrell, E. S. Fairbanks, R. P. Seraydarian, H. St. John, and R. E. Stockdale, Nucl. Fusion **26**, 543 (1986).
[9]R. C. Isler, L. E. Murray, E. C. Crume, C. E. Bush, J. L. Dunlap, P. H. Edmonds, S. Kasai, E. A. Lazarus, M. Murikami, G. H. Neilson, V. K. Pope, S. D. Scott, C. E. Thomas, and A. J. Wootton, Nucl. Fusion **23**, 1017 (1983).
[10]G. Pautasso, Ph. D. thesis, Georgia Institute of Technology, Georgia, January 1992; see also National Technical Information Document No. PB92177187 ("Analysis of a dedicated rotation experiment in TFTR," Georgia Tech Report GTFR-100). Copies may be ordered from National Technical Information Service, Springfield, Virginia 22161.
[11]G. A. Hallock, J. Mathew, W. C. Jennings, and R. L. Hickock, Phys. Rev. Lett. **56**, 1248 (1986).
[12]A. Kallenbach, H. M. Mayer, G. Fussmann, V. Mertens, U. Stroth, O. Vollmer, and the ASDEX Team, Plasma Phys. Controlled Fusion **33**, 595 (1991).
[13]A. Kallenbach (private communication, 1992).
[14]K. H. Burrell, R. J. Groebner, H. St. John, and R. P. Seraydarian, Nucl. Fusion **28**, 3 (1988).
[15]R. C. Isler, A. J. Wootton, L. E. Murray, J. D. Bell, C. E. Bush, A. Carnevali, P. H. Edmonds, D. P. Hutchinson, R. R. Kindsfather, R. A. Langley, E. A. Lazarus, C. H. Ma, J. K. Munroe, M. Murikami, G. H. Neilson, S. D. Scott, and C. E. Thomas, Nucl. Fusion **26**, 391 (1986).
[16]R. C. Isler and L. E. Murray, Appl. Phys. Lett. **42**, 355 (1983).
[17]W. M. Stacey, Nucl. Fusion **30**, 2453 (1990).
[18]S. Suckewer, H. P. Eubank, R. J. Goldston, E. Hinnov, and N. R. Sautoff, Phys. Rev. Lett. **43**, 207 (1979).
[19]S. D. Scott, P. H. Diamond, R. J. Fouck, R. J. Goldston, R. B. Howell, K. P. Jaehnig, G. Schilling, E. J. Synakowski, M. C. Zarnstorff, C. E. Bush, E. Frederickson, K. W. Hill, A. C. Janos, D. K. Mausfield, D. K. Owens, H. Park, G. Pautasso, A. T. Ramsey, J. Schivell, G. D. Tait, W. M. Tang, and G. Taylor, Phys. Rev. Lett. **64**, 531 (1990).
[20]W. M. Stacey, C. M. Ryu, and M. A. Malik, Nucl. Fusion **26**, 293 (1986).
[21]W. M. Stacey, Fusion Technol **23**, 157 (1993).
[22]W. M. Stacey and G. W. Neeley, Fusion Technol. **23**, 139 (1993).
[23]K. Ida, S. Hidekuma, M. Kojima, Y. Miura, S. Tsuji, K. Hoshino, M. Mori, N. Suzuki, and T. Yamauchi, Phys. Fluids B **4**, 2552 (1992).
[24]J. L. Terry, E. S. Marmar, K. I. Chen, and H. W. Moos, Phys. Rev. Lett. **39**, 1615 (1977).
[25]S. L. Allen, H. W. Moos, R. K. Richards, J. L. Terry, and E. S. Marmar, Nucl. Fusion **21**, 251 (1981).
[26]See National Technical Information Document No. PPPL-1430 [rapid scanning of spatial distribution of spectral line intensities in PLT tokamak, Princeton Plasma Physics Laboratory Report PPPL-1430 (1978)]. Copies may be ordered from National Technical Information Service Springfield, Virginia 22161.
[27]K. Brau, S. Suckewer, and S. K. Wong, Nucl. Fusion **23**, 1657 (1983).
[28]P. Smeulders, Nucl. Fusion **26**, 267 (1986).
[29]K. W. Wenzel, Bull. Am. Phys. Soc. **34**, 2153 (1989).
[30]C. S. Chang and R. D. Hazeltine, Nucl. Fusion **20**, 1397 (1980).
[31]K. H. Burrell, T. Ohkawa, and S. K. Wong, Phys. Rev. Lett. **47**, 511 (1981).
[32]C. T. Hsu and D. J. Sigmar, Plasma Phys. Controlled Fusion **32**, 499 (1990).
[33]W. M. Stacey and D. J. Sigmar, Phys. Fluids **27**, 2076 (1984).
[34]W. M. Stacey, A. W. Bailey, D. J. Sigmar, and K. C. Shaing, Nucl. Fusion **25**, 463 (1985).
[35]Y. B. Kim, P. H. Diamond, and R. J. Groebner, Phys. Fluids B **3**, 2050 (1991).
[36]J. W. Connor, S. C. Cowley, R. J. Hastie, and L. R. Pan, Plasma Phys. Controlled Fusion **29**, 919 (1987).
[37]W. M. Stacey, Plasma Phys. Controlled Fusion **31**, 1451 (1989).
[38]D. R. Jackson, Master's thesis, Georgia Institute of Technology, Georgia, 1992.